LAWRENCE
LIVERMORE
NATIONAL
LABORATORY

UCRL-JRNL-212927

Radiation-driven hydrodynamics of high-Z hohlraums on the National Ignition Facility

E. L. Dewald, L. J. Suter, O. L. Landen, B. R. Thomas, J. P. Holder, F. D. Lee, K. M. Campbell, J. Schein, F. A. Weber, D. G. Pellinen, M. B. Schneider, J. R. Celeste, J. W. McDonald, J. M. Foster, C. Niemann, B. K. Young, A. J. Mackinnon, S. Dixit, C. A. Haynam, M. J. Shaw, R. E. Turner, R. L. Kauffman, S. H. Glenzer, L. J. Atherton, R. E. Bonanno, S. N. Dixit, D. C. Eder, G. Holtmeier, D. H. Kalantar, A. E. Koniges, B. J. MacGowan, K. R. Manes, D. H. Munro, J. R. Murray, T. G. Parham, B. M. Van Wonterghem, R. J. Wallace, P. J. Wegner, P. K. Whitman, B. A. Hammel, E. I. Moses

June 14, 2005

Physical Review Letters

Radiation-driven hydrodynamics of high-Z hohlraums on the National Ignition Facility

E.L. Dewald, L.J. Suter, O.L. Landen, J.P. Holder, J. Schein, F.D. Lee, K.M. Campbell, F.A. Weber, D.G. Pellinen[#], M.B. Schneider, J.R. Celeste, J.W. McDonald, J.M. Foster*, C. Niemann, A.J. Mackinnon, S.H. Glenzer, B.K. Young, C.A. Haynam, M.J. Shaw, R.E. Turner, D. Froula, R.L. Kauffman, B.R. Thomas*, L.J. Atherton, R.E. Bonanno, S.N. Dixit, D.C. Eder, G. Holtmeier, D.H. Kalantar, A.E. Koniges, B.J. MacGowan, K.R. Manes, D.H. Munro, J.R. Murray, T.G. Parham, K. Piston, B.M. Van Wonterghem, R.J. Wallace, P.J. Wegner, P.K. Whitman, B.A. Hammel, and E.I. Moses

LLNL, P.O. Box 808, Livermore, CA 94550

[*]*AWE Aldermaston, Reading, RG7 4PR, United Kingdom*

[#]*Bechtel-Nevada, Livermore, CA 94550*

PACS numbers: 52.50.Jm, 52.40.Nk, 52.58.Ns, 52.70.Kz

Abstract:

The first hohlraum experiments on the National Ignition Facility using the initial four laser beams tested radiation temperature limits imposed by plasma filling. For a variety of hohlraum sizes and pulse lengths, the measured x-ray flux shows signatures of filling that coincide with hard x-ray emission from plasma streaming out of the hohlraum. These observations agree with hydrodynamic simulations and with an analytical model that includes hydrodynamic and coronal radiative losses. The modeling predicts radiation temperature limits with full NIF (1.8 MJ), greater, and of longer duration than required for ignition hohlraums.

The soft x-ray environment created in high-Z hohlraums heated by energetic laser beams, that enter the hohlraums through their Laser Entrance Holes (LEH), is used to drive fuel capsules in indirect-drive inertial confinement fusion (ICF) experiments and to drive physics packages in high energy density (HED) studies [1]. It has been shown analytically [2] that plasma filling by hohlraum wall ablation [3,4] imposes an upper bound to hohlraum x-ray production. Current simulations indicate that hohlraums used in ICF are optimized to drive a fusion capsule to ignition before reaching the x-ray production limits. On the other hand, many HED applications [5,6] require a long sustained soft x-ray drive [7,8]. These experiments will approach the limits in T_R-τ space, where T_R is the hohlraum peak radiation temperature and τ is the time at which the internal hohlraum radiation flux will begin to drop or roll-over, even before the laser pulse terminates. This occurs when the ablated hohlraum wall plasma reaches a density threshold that prevents the laser from propagating into the hohlraum due to absorption or backscattering. It was originally proposed [2] that this roll-over time τ is determined by laser-plasma instabilities when the plasma density approaches $0.1n_c$, where n_c [cm^{-3}]= $1.1\ 10^{21}$ /λ^2[μm^2] is the critical density for laser light of wavelength λ. However, hohlraum experiments with short laser pulse duration have performed properly well beyond the time at which they fill to $0.1n_c$ [9,10] indicating that a critical experimental test of hohlraum fill modeling is required for assessing long radiation drive options. In this paper we present results from experiments, numerical simulations and analytic modeling, demonstrating vacuum hohlraum performance with a sustained radiation drive over time scales consistent with a higher fill density limit.

The National Ignition Facility (NIF) that is currently under construction [11] is a 192 laser beam system that is designed to deliver up to 1.8 MJ of energy at a wavelength of λ_0

= 351 nm. The laser is designed for indirect drive ICF and will also be used for a variety of HED experiments. Recently, the first four laser beams were activated and experiments were performed successfully to study laser beam propagation in long scale plasmas with lengths of gas-filled ignition hohlraums [12]. In this study we present the first hohlraum experiments on the NIF that employ its unique capability to provide long, steady laser drives with variable pulse lengths, up to 20 ns. In these experiments constant power (flattop) laser pulses with 100 ps rise and fall times were used, with pulse lengths between 2 and 9 ns and energies between 5 and 17 kJ.

We used cylindrical Au hohlraums of various sizes with a single LEH and irradiated the hohlraum back wall with the four laser beams effectively forming an f/8 cone that propagates along the hohlraum axis (see Fig. 1a at 1 ns). Full aperture phase plates [13] and polarization smoothing [14] were installed on the laser beams providing a uniform intensity profile spot with a radial profile that is approximated by a n = 5 super-Gaussian with a 500 μm diameter (1/e points) with best focus placed at the LEH [12]. The Au hohlraum walls were 5 μm thick, backed by a 100 μm CH coating, allowing us to measure spatially resolved Au L-shell emission (> 9 keV) and to infer the hohlraum plasma fill dynamics [15]. We used a gated framing camera filtered for photon energies > 6keV with 100 μm Al, however when viewing side-on through the 5μm thick hohlraum Au walls the total filtering transmits > 9keV x rays.

The hohlraum radiation temperature was measured with temporal and spectral resolution through the LEH at 21.6° with an 18-channel absolutely calibrated soft x-ray power diagnostic, Dante [16]. Dante has a partial view of the initial laser spots on the hohlraum back wall and provides a measure of the radiation flux that includes both the primary laser-plasma emission and the re-emitting walls (see Fig. 2a). The total backscattered

laser energy measured with a Full Aperture Backscattering Station (FABS) [17], and a Near Backscattering Imager (NBI) [18] was < 0.6%. A static x-ray imager (SXI) confirmed that the beams propagate through the LEH without striking the outside walls of the hohlraum. Finally, the hot electron production inside the hohlraum was inferred from 20-100 keV absolutely calibrated x-ray spectra of the electron bremsstrahlung emission [19]. The measured hot electron fraction (temperature) was <~1% (30keV) in all hohlraums except the smallest, scale-¾ hohlraum where it was 4% (30keV), in good agreement with previous 3w experiments [1].

A series of experiments using 2 ns flattop pulses and variable laser energy in the 5-13 kJ range was first performed to measure the radiation temperature scaling with laser power and hohlraum size in a regime similar to previous hohlraums [9,10,20-23] where minimal plasma filling is expected. Measurements were compared to 2-D LASNEX radiation-hydrodynamics simulations [24] using the exact hohlraum geometry, measured laser power history [25], and a radially symmetric approximation to the combined spatial profile of the slightly diverging 4 beams. Table 1 shows measured and ***LASNEX*** predicted peak radiation temperatures for scale-1 (1.6 mm diameter, 1.5 mm long) and a scale-3/4 (1.2 mm diameter, 1.1 mm long) hohlraums with LEH sizes of 0.75 of the hohlraum diameter. The peak radiation temperature scales as expected with both the laser power and hohlraum size [21] and agrees with LASNEX simulations within the 2 % Dante radiation temperature error bar.

In the scale-1 2 ns pulse hohlraums the 9 keV side-on emission is localized at the back wall, indicating negligible plasma filling. Figure 1a shows that when irradiated by a longer 6 ns laser pulse the Au L-shell emission in the LEH region for a scale-1 hohlraum (0.8 mm LEH) eventually dominates as a result of plasma filling. We apply LASNEX

simulations to calculate the ablation from the gold hohlraum walls by soft x-rays and the cylindrically inward motion of the ablated plasma (Fig. 1c). First, the low-density ablation plasma moves into the beams path and is directly heated by the laser beams. This creates a high plasma pressure on the hohlraum axis retarding complete closure of the hohlraum, which is an important part of the hydrodynamics. Second, roll-over of the internal radiation temperature occurs at ~ 4 ns when the ablated plasma moving inward from the LEH begins to significantly absorb and refract the beam at the LEH. At this time, $n_e \sim 0.25 n_c$ at the center of the LEH and > 0.5nc at the outside of the beam. By 5.6ns the LEH plasma completely absorbs the laser beams. As a consequence, the hard x-ray radiation production migrates from the hohlraum back wall to the region of the LEH. This behavior is well reproduced by LASNEX post processed calculations of the Au L-shell emission (Fig. 1b) particularly the sudden transition from back wall to LEH dominated emission at ~ 4ns.

In addition to the scale-1 hohlraum irradiated with a 6 ns laser pulse, we performed long pulse experiments using larger, scale-3/2 hohlraums (2.4 mm diameter, 2.25 mm long, 1.4 mm LEH) demonstrating that our modeling correctly predicts the size scaling of plasma fill limits and the roll-over of the internal radiation temperature. With the same 6 ns laser pulse into the larger scale-3/2 hohlraum, the Au L-shell emission remains considerably stronger at the back wall than at the LEH, indicating that the hohlraum fill plasma density is moderate and that the laser still propagates into the hohlraum until the end of the laser pulse. However, when irradiating the same scale-3/2 hohlraum with a longer, 9 ns laser pulse of similar energy, we observe strong emission in the LEH starting at t = 7 ns.

Figure 2 shows the radiation temperature through the LEH T_{LEH} for the long pulse experiments measured by Dante, and simulated by LASNEX. Here T_{LEH} is the equivalent radiation temperature inferred from the absolute flux measured by Dante by using Stefan-Boltzmann law, i.e. Flux (W/sr)=$A_{LEH}\ \sigma T_{LEH}^4 \cos(21.6°)/\pi$, where A_{LEH} is the LEH area and σ is the Boltzmann constant. Figure 2 also shows the corresponding measured and simulated "M-band flux" (radiation > 2keV). Both the 9 ns scale-3/2 and the 6 ns scale-1 results (b and c) show two characteristic signatures of roll-over not seen in the 6 ns scale-3/2 result (a). Most prominent is the rise in Au M-band flux. These > 2keV x-rays are emitted by the hot LEH plasma that absorbs the laser beams and for which the Dante has a direct line-of-sight. In order to infer a roll-over time τ from our experiments, we use the time of the sudden rise in Au M-band flux. A less prominent but simultaneous signature of the roll-over is a sudden rise in the spectrally integrated $T_{LEH.}$ Further, Fig. 2 shows the calculated "internal T_R ", which is the radiation temperature that would drive an HED package located inside the hohlraum. This calculation shows "roll-over" at the time τ (Fig. 2b and c) when the LEH plasma is dense enough to absorb entirely the laser energy that coincides with the sudden rise in M-band emission and the rise in LEH temperature.

In addition to detailed numerical simulations, these results can be understood and extrapolated to higher laser energies and powers by applying a simple analytic model for radiation temperature limits. This model is based on the increased hydrodynamic losses and thin coronal radiative losses proportional to n_e^2 (n_e-electron density) [20] that occur when the laser absorption region migrates to the LEH as the hohlraum fills with plasma, leading to the roll-over in the internal radiation temperature. In our model these losses

become important at the LEH when the inverse bremsstrahlung absorption length λ_{IB} [26] in the laser heated LEH plasma becomes shorter than the LEH radius r:

$$\lambda_{IB} = T_e^{1.5}/200Z_H n_e^2 = 0.7r \quad (1)$$

where λ_{IB} and r are in units of cm, Coulomb logarithm is set to 7, n_e is the electron density in units of critical density n_c for the laser wavelength used, T_e is the electron temperature in keV, and Z_h is the average coronal charge state of the plasma fill. Equating the inverse Bremsstrahlung absorption to the electron conduction losses away from the laser heated channel inside the hohlraum sets one constraint on n_e and T_e [1]:

$$P_L = 0.14T_e^5/Z_h^2 n_e^2 \quad (2)$$

where P_L is the power of the flattop laser pulse in TW. The electron conduction losses are calculated according to the Spitzer model described in detail in [1] approximating the laser heated channel as spherical. Pressure balance between the laser heated plasma fill and the cold x-ray ablated Au wall with average ion density n_i and charge state Z defines another constraint on n_e and T_e [1]:

$$10n_eT_e = Zn_iT_R \quad (3)$$

where the factor of 10 accounts for the internal radiation temperature T_R that is expressed in units of heV, and n_i is in units of critical density. The average x-ray ablated ion density is proportional to the ablated wall areal mass density divided by the hohlraum radius R. For a Au cylindrical hohlraum wall [1] this gives us a relation between the ion density n_i and T_R:

$$n_i = 0.0007T_R^{1.86} t^{0.54}/R \quad (4)$$

where the hohlraum radius R is in cm and t is the time after the start of the laser drive. The average x-ray ablated Au ionization state Z as a function of the radiation temperature

T_R is given by $Z = 23T_R^{0.45}$ [1] and the average laser heated Au ionization state Z_H as a function of electron temperature T_e is given by $Z_H = 45T_e^{0.2}$ [27].

Another relation between the internal radiation temperature T_R, t and R is given by a traditional hohlraum power balance omitting thermal radiation losses out of the LEH which are lower than wall losses for the LEH sizes used here. This power balance assuming constant x-ray conversion efficiency (C.E.) of 75% and 100% absorbed laser energy is given by [1]:

$$P_L \propto T_R^4 R^2 (1 - \alpha) = 110 T_R^{3.3} R^2 / t^{0.4} \quad (5)$$

where the radiative wall loss fraction is $(1 - \alpha) = 0.45/T_R^{0.7}\, t^{0.4}$. This assumes a cylindrical halfraum with length L = 2R, as in the experiments described here. Combining equations (1)-(5) gives the roll-over radiation temperature $T_{max}=T_R(\tau)$ in terms of laser power, roll-over time τ and LEH radius r:

$$T_{max} = 1.0 P_L^{0.20}/r^{0.20}\tau^{0.07} = 1.0 E_L^{0.20}/r^{0.20}\tau^{0.27} \quad (6)$$

where T_{max} is in heV units, the flattop laser power (energy) P_L (E_L) is in TW (kJ), the filling time τ is in ns and the LEH radius r is in cm. The middle expression in Eq. (6) is applicable when the laser is power limited and the (right-hand) expression is applicable when the pulse length is long enough that the laser is energy limited. The relations (1)-(5) can be used to derive all significant hohlraum plasma parameters and the hohlraum size R. The optimum hohlraum size decreases for shorter fill (roll-over) times τ as smaller hohlraums will get hotter and fill faster with plasma.

As shown in Fig. 2, the simulated Dante (T_{LEH}) and internal (T_R) temperatures have similar values at the roll-over time, which allows us to compare T_{max} (Eq. (6)) directly to measured Dante temperature (T_{LEH}). Figure 3 plots the experimental Dante temperatures

(full circles) at the fill times τ and the corresponding T_{max} limits calculated with Eq. (6) (crosses) showing good agreement. Included are data points for the scale ¾ (Table 1) which showed significant LEH emission at the end of the pulse and for a smaller scale-3/8 hohlraum, heated by a 1.1 ns laser pulse [24]. By contrast, we calculate, as expected, that the T_{max} limits per Eq. (6) are significantly higher than the measured temperatures for the 2 ns short duration, scale-1 hohlraums exhibiting negligible plasma filling (see Table 1, scale 1), validating that for these combinations of laser power, pulse length and LEH size, higher temperatures could be reached using smaller hohlraums.

Figure 3 also shows analytical curves that describe the T_R limits (Eq. (6)) imposed by plasma filling for both the current NIF first quad experiment and for future experiments with the full NIF laser facility used to heat hohlraums with 192 beams through two LEHs. The two curves are calculated using Eq. (6) assuming a minimum LEH radius of 0.3 mm, dictated by the minimum NIF laser spot size and a maximum angle of incidence of 50°, and in the case of the full NIF hohlraum, an aspect ratio of L=3R. Extrapolating our analytic model predictions to full NIF hohlraum performance limits suggests a maximum achievable radiation temperature of T_{max} >700 eV.

In conclusion, we have demonstrated hohlraum performance limits consistent with simulations and analytic modeling for both low and high plasma filling conditions. The onset of significant plasma filling inferred by gated images of Au L-shell emission and the time dependence of the softer Au M-band flux measured by Dante were used to determine the roll-over time τ. The agreement between measurements and detailed LASNEX calculations constitute compelling evidence that the dynamics of bulk hohlraum filling is well understood. Furthermore, these observations agree with our analytical model that allows us to predict the radiation production limits for full NIF in

T_R-τ space. In our model the roll-over of the internal T_R occurs when hydrodynamic and coronal radiative losses out of the LEH become the dominant power loss contributors. The model can be easily extrapolated to other hohlraum geometries by modifying the constant in Eq. (4). For example, a spherical hohlraum [29] of equivalent surface area and LEH radius offers a larger volume (longer fill time), and hence T_{max} is about 5% higher. These are the first results that corroborate the limits imposed by hohlraum plasma filling in hohlraum radiation performance for indirect drive ICF and HED experiments.

This work would not have been possible without a large team which includes the NIF operations staff, the Bechtel Nevada LO calibrations staff, the target area staff and valuable contributions from G. Armstrong, D.E. Bower, S.C. Burkhart, R. Costa, C. Gates, J. Grinold, D. Hargrove, M. Hermann, S. Johnson, J. Kamperschroer, J. Kimbrough, T. Kohut, M. Landon, C. Marshall, J. Menapace, V. Rekow, M. Rhodes, V. Roberts, A. Warrick, P. Watts, and P.E. Young. The authors would also like to thank M-C Monteil, CEA, France, and R.M. Stevenson, AWE, for valuable discussions. This work was performed under the auspices of the U.S. Department of Energy by the University of California, Lawrence Livermore National Laboratory under Contract No. W-7405-ENG-48.

References

[1] J.D. Lindl, Phys. Plasmas **2**, 3933 (1995), J.D. Lindl et al., Phys. Plasmas **11**, 339 (2004).

[2] B. Thomas, AWE, private communication, 1995.

[3] G.D. Tsakiris and R. Sigel, Phys. Rev. A **38**, 5769 (1988).

[4] R.M. Stevenson et al., Phys. Rev. Lett. **94**, 055006 (2005).

[5] J. Massen et al., Phys. Rev. E **50**, 5130 (1994).

[6] A. Benuzzi et al., Phys. Rev E **54**, 2162 (1996).

[7] B. Remington et al., Metallurgical and Mat. Trans. A, **35A**, 2587 (2004).

[8] C.A. Back et al., Phys. Rev. Lett. **84**, 274 (2000).

[9] S.H. Glenzer et al., Phys. Rev. Lett. **80**, 2845 (1998).

[10] E. Dattolo et al., Phys. Plasmas **8**, 260 (2001).

[11] G.H. Miller, E.I. Moses and C.R. Wuest, Nucl. Fusion **44,** 228 (2004).

[12] S.H. Glenzer et al., Nucl. Fusion **44**, 185 (2004).

[13] J.A. Menapace, S.N. Dixit, F.Y. Genin, W.F. Brocious, Proc. Spie **5273**, 220 (2003).

[14] D. H. Munro, S. N. Dixit, A. B. Langdon, J. R. Murray, Appl. Opt. **43**, 6639 (2004).

[15] L.J. Suter et al., Rev. Sci. Instrum. **68**, 838 (1997).

[16] E.L. Dewald et al., Rev. Sci. Instrum. **75**, 3759 (2004).

[17] D. Froula et al., Rev. Sci. Instrum. **75**, 4168 (2004).

[18] A.J. Mackinnon et al., Rev. Sci. Instrum. **75**, 4183 (2004).

[19] J.W. McDonald et al., Rev. Sci. Instrum. **75**, 3753 (2004).

[20] L.J. Suter et al., Phys. Plasmas **3,** 2057 (1996).

[21] R. Sigel et al., Phys. Rev. Lett. **65**, 587 (1990).

[22] J. Massen, G.D. Tsakiris and R. Sigel, Phys. Rev. E **48**, 2073 (1993).

[23] K. Eidmann et al., Phys. Rev. E **52**, 6703 (1995).

[24] G.B. Zimmerman and W.L. Kruer, Comm. Plasma Phys. Contr. Fusion **2**, 51 (1975).

[25] L.J. Suter et al., Phys. Rev. Lett **73**, 2328 (1994).

[26] T.W. Johnston and J.M. Dawson, Phys. Fluids **16**, 722 (1973).

[27] R.W. Lee *et. al*., JQSRT **58,** 737 (1997).

[28] D. Hinkel et al., Phys. Plasmas, **12**, 056305 (2005).

[29] J.M. Wallace. et. al., Phys. Rev. Lett. **82**, 3807 (1999).

Table and Figure captions

Table 1 Peak radiation temperature measured with Dante and calculated for 2 ns flattop laser pulses vs. hohlraum scale and laser power.

Figure 1 Side-on hard x-ray gated images (a) measured and (b) calculated in scale-1 hohlraum heated by 2.7 TW, 6 ns laser pulse; experiment layout and laser beams are schematically shown. (c) Cross-section of electron density profiles and laser ray propagation calculated with 2D LASNEX code. .

Figure 2 Radiation temperature history as measured by Dante through LEH (continuous thick line) and as simulated by LASNEX (full squares). Circles are predicted internal radiation temperatures. Measured (continuous thin line) and calculated (triangles) M-band (>2 keV) flux are plotted on RHS scale. (a) scale-3/2 hohlraum driven by 2.7 TW in 6 ns, (b) scale-3/2 driven by 1.9 TW in 9 ns and (c) scale-1 driven by 2.7 TW in 6 ns flattop laser pulse. Dante view of typical hohlraum target with initial laser spots on the wall shown as dark circle shown as insert on a).

Figure 3 Dante measured temperatures T_{LEH} at the roll-over time τ and the corresponding analytical limits (crosses) calculated with Eq. (6) using experimental values of LEH radius r and laser power. Continuous and dashed black lines are Eq. (6) analytic model limits for a constant LEH radius r = 0.3 mm for 9 TW, 16 kJ 1 quad NIF halfraums and for 600 TW, 1.8 MJ NIF hohlraum.

Table 1

Laser Power (TW)	Scale	Peak Dante Tr (eV)	Calculated Peak "Dante" Tr
2.5	1	188	185
4.8	1	221	218
6.6	1	240	236
6.7	0.75	276	277

Figure 1

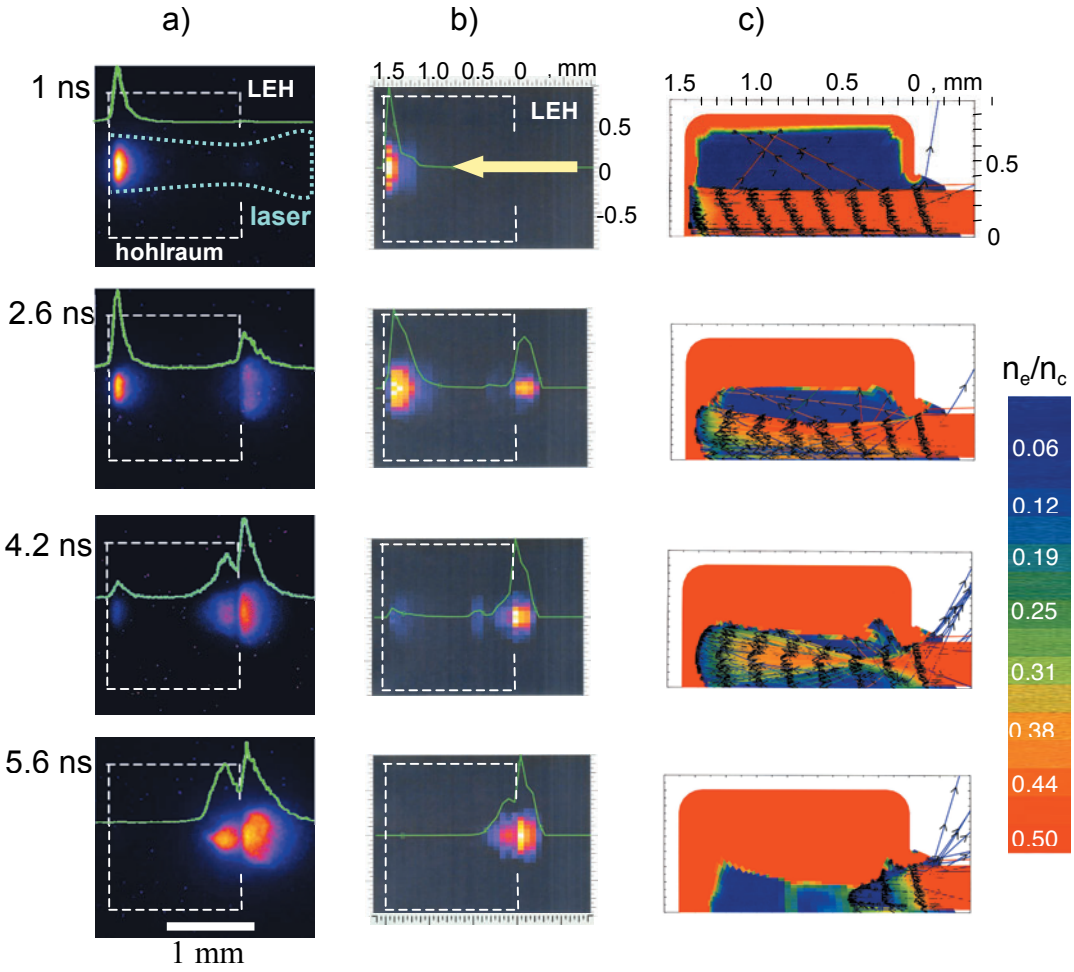
a)
b)
c)
1 ns
2.6 ns
4.2 ns
5.6 ns
LEH
laser
hohlraum
1.5 1.0 0.5 0 mm
0.5
0
-0.5
1.5 1.0 0.5 0 , mm
0.5
0
n_e/n_c
0.06
0.12
0.19
0.25
0.31
0.38
0.44
0.50
1 mm

Figure 2

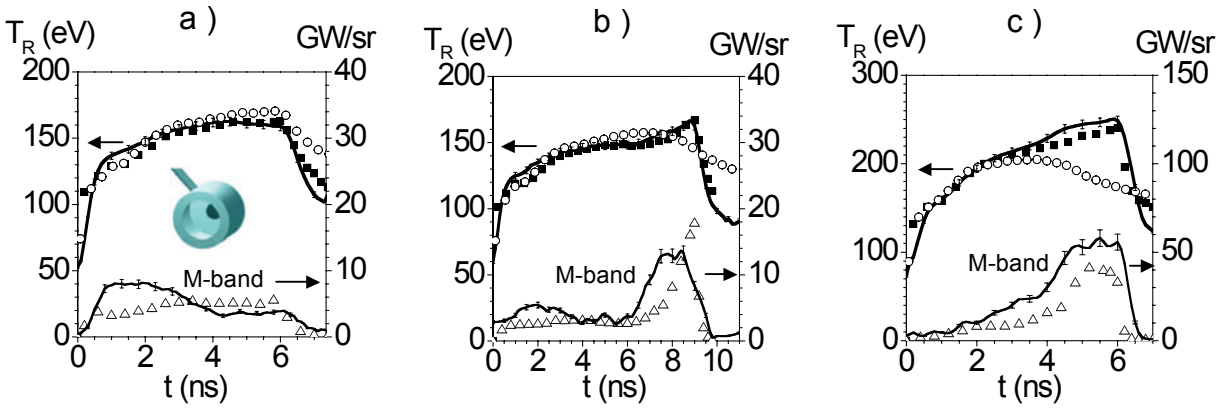

Figure 3

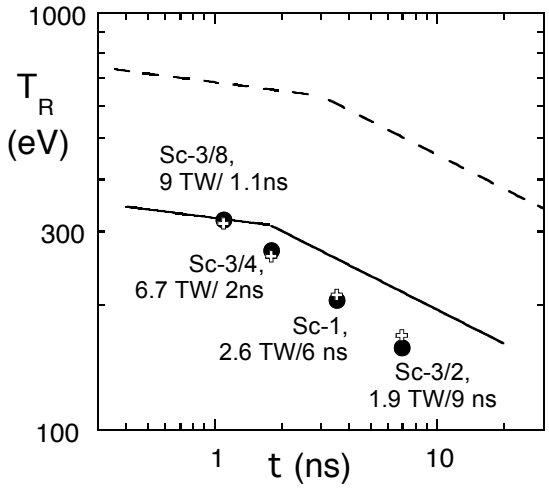
1000
T_R
(eV)
300
100
Sc-3/8,
9 TW/ 1.1ns
Sc-3/4,
6.7 TW/ 2ns
Sc-1,
2.6 TW/6 ns
Sc-3/2,
1.9 TW/9 ns
1
t (ns)
10